34th Annual International Conference of the IEEE EMBS
San Diego, California USA, 28 August - 1 September, 2012

A Shape Constrained Parametric Active Contour Model for Breast Contour Detection*

Juhun Lee, *Student Member*, *IEEE,* Gautam S. Muralidhar, *Student Member*, *IEEE*,
Gregory P. Reece, and Mia K. Markey, *Senior Member*, *IEEE*

Abstract—**Quantitative measures of breast morphology can help a breast cancer survivor to understand outcomes of reconstructive surgeries. One bottleneck of quantifying breast morphology is that there are only a few reliable automation algorithms for detecting the breast contour. This study proposes a novel approach for detecting the breast contour, which is based on a parametric active contour model. In addition to employing the traditional parametric active contour model, the proposed approach enforces a mathematical shape constraint based on the catenary curve, which has been previously shown to capture the overall shape of the breast contour reliably [1]. The mathematical shape constraint regulates the evolution of the active contour and helps the contour evolve towards the breast, while minimizing the undesired effects of other structures such as, the nipple/areola and scars. The efficacy of the proposed approach was evaluated on anterior posterior photographs of women who underwent or were scheduled for breast reconstruction surgery including autologous tissue reconstruction. The proposed algorithm shows promising results for detecting the breast contour.**

I. INTRODUCTION

Due to improvements in early breast cancer detection techniques and treatments, the mortality rate of breast cancer has decreased significantly since 1990 [2-4]. Consequently, there is increasing emphasis on restoring breast cancer survivors' quality of life. Breast reconstruction surgical procedures help surviving cancer patients psychologically adjust by restoring their breast(s). Breast reconstruction is not a single step procedure; there are multiple options available for the patient to choose from and they usually consist of multiple surgeries and revisions to achieve a desirable outcome. Although patients' surgeons help them with these decisions, breast cancer survivors are often still overwhelmed by uncertainties during the process of selecting reconstruction options. Quantitative measures of breast morphology may help breast cancer survivors to elucidate such uncertainties by providing them a systematic methodology to understand outcomes of reconstructive options.

There are many previous studies that have introduced measures for quantifying breast morphology, e.g., [1, 5-9]. Delineating the breast contour is an important precursor for computing many measures of breast morphology. One bottleneck in quantifying breast morphology is that there are only a few reliable algorithms for detecting breast contour. To the best our knowledge, only one research group has introduced an algorithm for automatically tracing the breast contour. In their work [10], Dijkstra's shortest path algorithm was applied on the gradient map of patients' clinical photographs with shape priors using parabola, ellipse (parametric priors), or previously outlined breast contour examples (non-parametric priors) on the path. Although their algorithm showed acceptable results on a dataset comprised of clinical photographs of 120 patients who underwent breast conservation therapy, the algorithm has two key limitations for our application: 1) any strong gradient changes around the breast contour such as the nipple/areola or scars due to surgery can cause the algorithm to fail since it is based solely on the image gradient, and 2) it has not been validated on clinical photographs of patients who underwent breast reconstruction.

In this study, we propose a novel approach for detecting the breast contour, which is based on a parametric active contour model. Active contours or snakes have been used for many computer vision and image processing tasks such as segmentation or tracking objects since it was first proposed by Kass et al [11]. An active contour is a parametric curve that deforms to the object of interest by minimizing an energy functional with constraints on the curve evolution. In a traditional active contour model, the energy functional is usually comprised of internal and external force terms. The internal force terms help the contour retain its smoothness and tautness, while the external force influences the contour to deform towards the object of interest. The edge map of an image is a popular choice for the external force. However, the use of an edge map alone as the external force does not suffice when it comes to detecting the breast contour since the presence of other structures, such as nipple/areola region and scars can contribute to external force, thereby hindering the accurate delineation of the breast contour. To overcome this problem, the traditional active contour model was augmented with a mathematical shape constraint that was

*This study was supported in part by grant RSGPB-09-157-01-CPPB from the American Cancer Society and grant R01CA143190-01A1 from the National Institutes of Health.

J. Lee is with the Department of Electrical and Computer Engineering, The University of Texas at Austin, Austin, TX 78712, USA, and with the Department of Plastic Surgery, The University of Texas MD Anderson Cancer Center, Houston, TX 77030, USA (phone: 512-471-8660; fax: 512-471-0616; e-mail: juhunlee@utexas.edu).

G. S. Muralidhar is with the Department of Biomedical Engineering, The University of Texas at Austin, Austin, TX 78712, USA, and with the Department of Diagnostic Radiology, The University of Texas MD Anderson Cancer Center, Houston, TX 77030, USA (e-mail: gautam.sm@utexas.edu).

G. P. Reece is with the Department of Plastic Surgery, The University of Texas MD Anderson Cancer Center, Houston, TX 77030, USA (e-mail: greece@mdanderson.org).

M. K. Markey is with the Department of Biomedical Engineering, The University of Texas at Austin, Austin, TX 78712, USA, and with the Department of Imaging Physics, The University of Texas MD Anderson Cancer Center, Houston, TX 77030, USA (e-mail: mia.markey@austin.utexas.edu).

based on the prior knowledge of the breast morphology. This approach is similar to that introduced in the work of Ray et al. [12] for tracking Leukocytes *in Vivo*. In their study, the prior knowledge of the shape of Leukocytes, which are approximately elliptic, was incorporated as an additional external force in the active contour framework. In this study, we used the catenary curve as the shape constraint for the active contour model. The catenary has been previously shown to capture the overall curvature of breast contour reliably [1]. The mathematical shape constraint regulates the evolution of the active contour and helps the contour to evolve towards the breast contour. We describe the proposed approach next.

II. Proposed Approach

A. Shape Constrained Parametric Active Contour

An active contour is a parametric curve $v(s)=[x(s),y(s)]^T, s\in[0,1]$ that evolves to minimize the following energy functional

$$E=\int_0^1\left[\frac{1}{2}\left(w_1 v_s(s)+w_2 v_{ss}(s)\right)^2+E_{ext}\right]ds, \tag{1}$$

where v_s(s) and v_{ss}(s) are the first and second derivatives of v(s) with respect to s, respectively, and w_1 and w_2 are associated weights for the derivatives to control the continuity and curvature (tautness) of the contour. E_{ext} is the external energy, which represents the external forces that influence the curve evolution.

In the proposed approach, an image with oriented structures enhanced was used for E_{ext}, since the breast contour manifests as a strong, oriented structure in the image. To obtain the orientation-enhanced image, we employed a quadrature pair comprised of the steerable fourth derivative of a 2D gaussian and its Hilbert transform, respectively [13]. The orientation-enhanced image was embedded within the Vector Field Convolution (VFC) framework [14] to make the external energy term provide a large capture range and also make it robust to noise.

To incorporate prior knowledge of the breast contour into our model, we introduce a shape constraint $F_{shape}=\left(v(s)-v_c(s)\right)^2,\ s\in[0,1]$, where $v_c(s)$ is defined as

$$v_c(s)=\begin{bmatrix}\cos\theta & -\sin\theta\\ \sin\theta & \cos\theta\end{bmatrix}\begin{bmatrix}\alpha\cdot 2(s-1)+b\\ -\alpha\cosh\left(2(s-1)\right)+c\end{bmatrix}. \tag{2}$$

Equation (2) represents the rotated version of a catenary curve, which captures the overall curvature of the breast contour reliably [1]. In (2), b and c are the offset of the x-axis and y-axis, respectively, and α is the ratio of the tension to the weight applied to each point on the curve. The rotation parameter, θ, captures the angle between the breast contour and the imaginary horizontal line. The term 2(s-1) was introduced to make the catenary curve symmetric about the $s=0$ line. We used the parametric representation of the catenary curve since the parameters in (2) can be used to quantify the breast morphology (e.g., α is the quantitative measure of overall breast curvature [1]). We augmented the shape constraint with the balloon inflation force $F_{balloon}$ introduced in the balloon model [15], which is simply the unit normal vector of each vertex in the active contour. This was done to prevent the contour from evolving towards a trivial local optima such as collapsing to a point.

The resulting Euler-Lagrange equation to minimize the energy functional (1) is given as

$$w_1 v_{ss}(s)-w_2 v_{ssss}(s)-\nabla E_{ext}\left(v(s)\right)-\lambda F_{shape}+\tau F_{balloon}=0, \tag{3}$$

which can be represented as

$$F_{int}+F_{ext}=0, \tag{4}$$

where $F_{\text{int}}=w_1 v_{ss}(s)-w_2 v_{ssss}(s)$ is the internal force needed to retain the continuity and tautness of the contour, and $F_{ext}=-\nabla E_{ext}\left(v(s)\right)-\lambda F_{shape}+\tau F_{balloon}$, is the external force needed to attract the contour to the breast contour, where λ and τ are weights to control the effect of the shape prior and the inflation force.

To solve (3), the contour v(s) is considered as a function of time t. The steady state solution of (3) can be found using the gradient descent equation as follows

$$\frac{\partial v(s,t)}{\partial t}=F_{int}\left(v(s,t)\right)+F_{ext}\left(v(s,t)\right). \tag{5}$$

The initial contour for (5) is defined as $v(s,0)=v_c(s,\alpha_0,b_0,c_0,\theta_0)$ where α_0, b_0, c_0 and θ_0 are the initial values for the parameters in (2). This initial *open* contour was used as an approximation of the breast contour.

B. Numerical Implementation

Let $S_p=\left[w_1,w_2,\lambda,\tau\right]$ denote the static parameter set - the parameters that are held constant during each iteration of the algorithm. The values of the parameters in S_p were empirically set to $\left[0.05,0.15,0.1,0.2\right]$. Let $D_p=\left[\alpha,b,c,\theta\right]$ denote the active catenary parameter set, which are updated in each iteration. We set the initial value of [α,θ] to [70 20] for the patient's right breast contour and to [70 -20] for the patient's left breast contour. The initial values for [b, c] were computed from the location of Anterior Axilliary Point (AAP), which is defined as a point in the top portion of the anterior axillary fat pad, which starts from the very top of anterior axillary fat pad ($\text{AAP}_{\text{upper}}$) to the junction of the anterior axillary fad pad and the breast ($\text{AAP}_{\text{lower}}$) (Fig. 1.A). The initial values [b, c] were set to make one end of the active contour to be located at the AAP. We selected the AAP for the initialization of [b, c] because of the following reasons: 1) it is located close to the breast contour and some AAPs are the end point of the breast contour, 2) unlike other fiducial points, such as the nipple or areola, its location is not as affected by the breast reconstruction or oncologic surgery. For this study, the first author (J.L.) manually located the AAPs on all patients' photographs. For most cases, the AAP is located at the $\text{AAP}_{\text{upper}}$. For patients with severely ptotic

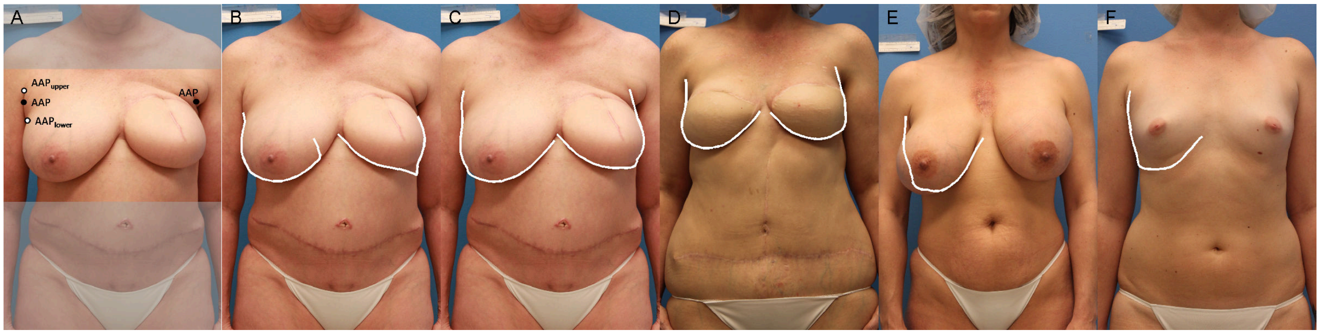

Figure 1. **A:** Top 20% and bottom 40% of the image were masked out since those regionsare not expected to contain the patient's breasts given the standard pose used. Anterior Axillary Points (AAP) were manually located on the image. The AAP is defined as a point in the top portion of the anterior axillary fat pad, which starts from the very top of anterior axillary fat pad (AAP_{upper}) to the junction of the anterior axillary fad pad and the breast (AAP_{lower}) **B:** The result of the traditional balloon active contour algorithm without the catenary shape constraint. Without the shape constraint, the active contour is unable to delinearate the breast contour properly. **C-D:** Examples of success cases. **E-F:**Examples of failure cases. In **E**, the proposed algorithmfailed due to the failure of the nipple detection method. In **F**, this failure was due to the weak steerable filter response of the breast contour. Since the shadow under the breast contour creates a stronger filter response, the active contour is attracted to the edge of shadow, not the edge of the breast contour.

breasts, the location of the AAP was moved close to the AAP_{lower}. If desired, this step could be easily automated as shown by Cardoso et al. [10].

The pseudocode of the algorithm is:

- WHILE $\sum_i \left| v(i,t) - v(i,t-1) \right| < 0.1$
  - Update $v(i,t)$ by solving (5)
  - Update $[\alpha, b, c, \theta]$ from $v(i,t)$ by solving (2) in least square sense [1]
- END

After the algorithm terminates its iterations with the initial static parameter set, the algorithm is applied again with a lower weight on the shape constraint, i.e., smaller λ value, to make the active contour capture the local variation of breast contour better. At this step, we set λ value as 0.05 and the other static parameters remain unchanged.

III. Experimental Evaluation

A. Dataset

The study population for this paper consists of women aged 21 or older who underwent or were scheduled for breast reconstruction surgery from January 1, 2010 to December 31, 2011 at The University of Texas MD Anderson Cancer Center. A Canon EOS REBEL T1i (Canon, USA) was used to obtain anterior posterior (AP) images of 46 patients (79 breasts). Of the 79 breasts, 56 breasts were either healthy or untreated breasts and 23 breasts were transverse rectus abdominis myocutaneous (TRAM) reconstructed breasts.

All photographs in the dataset were first rescaled to the size of 1188 x 792 pixels in order to increase the speed of the proposed algorithm without compromising its performance. Then, the top 20% and bottom 40% of the patient in the image, which are not expected to contain the patient's breasts given the standardized posed used, were masked out automatically to minimize the changes of false positive detection. These masked out regions were verified with the randomly selected subset of the dataset (N = 6).

The nipple/areola is one of the most salient structures of the breast, which can distract most gradient-based breast contour detection algorithms. In order to minimize possible false detection, we automatically located the nipple/areola region and created a patch, which is used for masking the nipple/areola location in the external force map. We employed the method described in [16] to locate the nipple/areola region in the photograph. The Q channel image of the YIQ color space of photographs is first thresholded using the 40% of the maximum Q channel intensity of the image. Then, the resulting binary image is dilated and eroded using a 'disk' structural element with radius of 3 pixels, to find the nipple/areola region. After that, the preprocessed image is converted to grayscale before subsequent processing to detect the breast contour.

B. Results

Fig. 1.C and Fig. 1.B show the results of the proposed algorithm with and without the shape constraint, respectively, to detect the contours of untreated and TRAM reconstructed breast. This figure demonstrates that the shape constraint based on the catenary curve helps the active contour to maintain its form close to the typical shape of the breast contour. Specifically, the shape constraint based on the catenary curve restricts two ends of the active contour to deviate from the breast contour. Moreover, it ensures the middle of the active contour to have smooth curvature, which is typically observed from the actual breast contour.

Two non-clinical observers (J.L. and G.S.M.) examined the outcomes of the proposed algorithm and made a choice whether the outcome was successful or not. The cases for which both observers agreed that the contour was detected correctly were treated as successes. Overall, the proposed algorithm accurately detected the healthy or untreated breasts (84%) and TRAM reconstructed breasts (91%). Most failures were due to the weak steerable filter response of the breast contour. Since the lower breast contour is not obvious for those cases (Fig. 1.F) its filter response is not strong enough to attract the active contour. Some other failures (Fig. 1.E) were due to the failure of the nipple/areola detection. One failure was due to moles located close to breast contour, which distracts the active contour to converge to the breast contour.

For the successful cases (i.e., the case on which both observers felt that the contour had been accurately located), we evaluated the accuracy of the proposed algorithm. For this, the first author (J.L.) manually traced the breast contour of the success cases using a stylus and a tablet computer, prior to applying the proposed algorithm to the images. Table I shows the accuracy of the proposed algorithm with respect to the average distance (error) between the detected breast contour and the manually traced contour. The average errors across the images were less than 9.4 pixels (approximately 0.67 *cm*). The error was similar for untreated and TRAM reconstructed breasts. The biggest contribution to the error of the proposed algorithm was from the end point of the automated contour. However, the effect of such an error arising from the end-points of the contour is insignificant when it comes to quantitatively measuring breast morphology factors such as curvature [1], since these factors employ the middle portion of the breast contour.

While it is not possible to directly compare our study to prior studies on breast contour detection since the algorithms were deployed on different datasets, we provide a brief discussion for reference. On a data set of women who underwent breast conservation therapy, Cardoso et al. [10] presented an algorithm that located the breast contour with error of around 0.3 *cm*.

TABLE I. QUANTIATIVE EVALUATION

Avg. Error	Healthy or Untreated			TRAM reconstructed		
	Mean	***Std***	**[*Min Max*]**	***Mean***	***Std***	**[*Min Max*]**
in pixel	9.4	3.9	[4.9 24.4]	8	2.2	[4.8 12.9]
in cm	0.67	0.28	[0.35 1.74]	0.58	0.24	[0.34 0.92]

IV. CONCLUSION

The proposed algorithm using active contour with the shape constraint shows promising results for detecting the breast contour of untreated breast and TRAM reconstructed breasts. In future work, we will validate the algorithm with the dataset with larger sample size of healthy and TRAM reconstructed breasts as well as additional types of reconstruction, e.g., tissue expander / implant.

ACKNOWLEDGMENT

The authors wish to recognize former and current Plastic Surgeons of The University of Texas MD Anderson Cancer Center for their support and/or contribution of patients to this series: Drs. Charles E. Butler, David W. Chang, Donald P. Baumann, Elisabeth K. Beahm, Geoffrey L. Robb, Justin M. Sacks, Jesse C. Selber, Melissa A. Crosby, Mark T. Villa, Matthew M. Hanasono, Patrick B. Garvey, Pierre M. Chevray, Roman Skoracki, and Steven J. Kronowitz, Scott D. Oates. We also acknowledge June Weston and D. Samantha Picraux for their efforts in data collection. We wish to thank Francis Carter for his support in management of the data.

REFERENCES

[1] J. Lee, S. Chen, G. Reece, M. Crosby, E. Beahm, and M. Markey, "A Novel Quantitative Measure of Breast Curvature Based on Catenary," *Biomedical Engineering, IEEE Transactions on,* vol. PP, pp. 1-1, 2012.

[2] "Cancer Facts and Figures 2012," American Cancer Society2012.

[3] A. Khoo, S. S. Kroll, G. P. Reece, M. J. Miller, G. R. Evans, G. L. Robb, B. J. Baldwin, B. G. Wang, and M. A. Schusterman, "A comparison of resource costs of immediate and delayed breast reconstruction," *Plastic and Reconstructive Surgery,* vol. 101, pp. 964-968, 1998.

[4] S. S. Kroll, G. R. Evans, G. P. Reece, M. J. Miller, G. L. Robb, B. J. Baldwin, and M. A. Schusterman, "Comparison of resource costs of free and conventional TRAM flap breast reconstruction," *Plastic & Reconstructive Surgery,* vol. 98, pp. 74-7, 1996.

[5] M. S. Kim, G. P. Reece, E. K. Beahm, M. J. Miller, E. Neely Atkinson, and M. K. Markey, "Objective assessment of aesthetic outcomes of breast cancer treatment: measuring ptosis from clinical photographs," *Comput Biol Med,* vol. 37, pp. 49-59, Jan 2007.

[6] R. D. Pezner, M. P. Patterson, L. R. Hill, N. Vora, K. R. Desai, J. O. Archambeau, and J. A. Lipsett, "Breast retraction assessment: an objective evaluation of cosmetic results of patients treated conservatively for breast cancer," *Int. J. Rad. Oncol. Bio. Phy.,* vol. 11, pp. 575-8, 1985.

[7] V. Sacchini, A. Luini, S. Tana, L. Lozza, V. Galimberti, M. Merson, R. Agresti, P. Veronesi, and M. Greco, "Quantitative and qualitative cosmetic evaluation after conservative treatment for breast cancer," *Eu. J. Cancer,* vol. 27, pp. 1395-400, 1991.

[8] J. S. Cardoso and M. J. Cardoso, "Towards an intelligent medical system for the aesthetic evaluation of breast cancer conservative treatment," *Artificial Intelligence In Medicine,* vol. 40, pp. 115-126, 2007.

[9] E. Van Limbergen, E. van der Schueren, and K. Van Tongelen, "Cosmetic evaluation of breast conserving treatment for mammary cancer. 1. Proposal of a quantitative scoring system," *Radiother. Oncol.,* vol. 16, pp. 159-67, 1989.

[10] J. S. Cardoso, R. Sousa, L. F. Teixeira, and M. J. Cardoso, "Breast Contour Detection with Stable Paths," in *Biomedical Engineering Systems and Technologies*. vol. 25, A. Fred, J. Filipe, and H. Gamboa, Eds., ed: Springer Berlin Heidelberg, 2009, pp. 439-452.

[11] M. Kass, A. Witkin, and D. Terzopoulos, "Snakes: active contour models," *International Journal of Computer Vision,* vol. 1, pp. 321-331, 1987.

[12] N. Ray, S. T. Acton, and K. Ley, "Tracking leukocytes in vivo with shape and size constrained active contours," *Medical Imaging, IEEE Transactions on,* vol. 21, pp. 1222-1235, 2002.

[13] W. T. Freeman and E. H. Adelson, "The Design and Use of Steerable Filters," *IEEE Trans. Pattern Anal. Mach. Intell.,* vol. 13, pp. 891-906, 1991.

[14] B. Li and S. T. Acton, "Active contour external force using vector field convolution for image segmentation," *IEEE Transactions on Image Processing,* vol. 16, pp. 2096-2106, 2007.

[15] L. D. Cohen, "On active contour models and balloons," *CVGIP: Image Understanding,* vol. 53, pp. 211-218, 1991.

[16] M. Dabeer, E. Kim, G. P. Reece, F. Merchant, M. A. Crosby, E. K. Beahm, and M. K. Markey, "Automatic calculation of symmetry measure on clinical photographs," *Journal of Evaluation in Clinical Practice,* vol. 17, pp. 1129-1136, 2011.